Ain Shams Engineering Journal xxx (xxxx) xxx

Contents lists available at ScienceDirect

Ain Shams Engineering Journal

journal homepage: www.sciencedirect.com

Electrical Engineering

A modified energy management scheme to support phase balancing in grid interfaced photovoltaic/fuel cell system

Mustafa İnci [a,*], Mehmet Selim Aygen [b]

[a] İskenderun Technical University, Faculty of Engineering and Natural Sciences, Mechatronics Engineering, 31200 İskenderun, Hatay, Turkey
[b] Gazi University, Faculty of Technology, Electrical and Electronics Engineering, 06560 Yenimahalle, Ankara, Turkey

ARTICLE INFO

Article history:
Received 9 July 2020
Revised 5 November 2020
Accepted 18 December 2020
Available online xxxx

Keywords:
Phase balancing
Hybrid system
Grid-connected
Unbalanced loads
Unbalanced currents

ABSTRACT

This paper presents improved energy management for grid-inverter of a hybrid photovoltaic (PV)/fuel cell (FC) energy system with unbalanced sensitive loads. In the system, unbalanced loads draw unbalanced currents at each phase and consume power from energy units at different levels. This condition makes the grid unbalanced, which cannot be compensated by a conventional energy management controller used in grid inverters. For this, a phase balancing control method is proposed in order to improve the grid quality under unbalanced loading conditions. The proposed method calculates power differentiation values based on multiple-frame αβ/dq transform instead of abc/dq transform in the conventional method. Thus, it eliminates negative & zero sequence components in addition to power flow control. Under unbalanced loading conditions, the proposed method removes the deficiency of the conventional energy management method which generates the symmetrical current references to trigger the switching elements of the inverter. In performance results, the system with unbalanced loads is tested for different case studies, which supply different power from energy units to grids. The results show that the proposed method provides power balancing at the grid-side and eliminates negative & zero sequence components at grid-side currents.

1. Introduction

1.1. Overview

Renewable energy technologies are becoming increasingly popular for residential and utility-scale applications with technological advancements. In order to meet the electrical power demand, renewable energy sources are used in the electrical grid integration implementations for additional power supply [1]. The integration of two or more renewable energy sources with utility-grids is briefly defined as grid-connected hybrid energy systems [2–4]. In these systems, excess electrical energy is transferred to the grid, or the needed electrical power is completed from the grid to feed local load banks. This means that the electricity produced by the hybrid system can either be used directly (which is suitable for illumination, heating and other devices in buildings) or be commercialized to the electrical distribution companies [5–7].

In renewable energy technologies, hybrid energy systems, including photovoltaics (PVs) and fuel cells (FCs), are broad and desirable according to easy operation, simple working and environmental sources [8,9]. Moreover, PVs and FCs ensure a good solution for power balancing and voltage/frequency regulation in comparison to the intermittency of a wind turbine in power outputs [6,10]. These structures should be cautiously organized and handled to supply optimized active power from renewable energy systems to utility-grids [11–13]. Thus, the energy generation units are placed in an electrical line to strengthen the grid power, thus decreasing the instantaneous oscillations and enhancing system stability/performance [14]. In this regard, the grid-connected hybrid systems provide a collective power exchange from energy units to local loads/grids.

* Corresponding author at: İskenderun Technical University, Mechatronics Engineering, 31200 İskenderun, Hatay, Turkey.
E-mail addresses: mustafa.inci@iste.edu.tr (M. İnci), msaaygen@gmail.com (M.S. Aygen).

Peer review under responsibility of Ain Shams University.

Production and hosting by Elsevier

https://doi.org/10.1016/j.asej.2020.12.018
2090-4479/

Please cite this article as: M. İnci and Mehmet Selim Aygen, A modified energy management scheme to support phase balancing in grid interfaced photovoltaic/fuel cell system, Ain Shams Engineering Journal, https://doi.org/10.1016/j.asej.2020.12.018

Nomenclature

AC	Alternating current
DC	Direct current
D1	Duty cycle of FC-side switch
D2	Duty cycle of PV-side switch
FC	Fuel cell
IEEE	Institute of Electrical and Electronics Engineers
I_{sc}	Output current in PV panel
I_{fc}	Output current in FC stack
$I_{load,n}$	Load current (n = a,b,c)
$I_{dc,ref}$	Average current reference
$I_{ref,n}$	Reference value for switching (n = a,b,c)
I_{dn}	Direct-component of system currents
I_{qn}	Quadrature-component of system currents
$I_{dif,n}$	Differentiation value of current (n = a,b,c)
MPPT	Maximum power point tracking
N	Number of cells in an FC
PEMFC	Proton exchange membrane fuel cell
PLL	Phase locked loop
PI	Proportional-integral
PWM	Pulse width modulation
PV	Photovoltaics
P&O	Perturb and observe
$P_{grid,n}$	Grid-side power
$P_{load,n}$	Load-side power
$P_{sys,n}$	Supplied power from PV/FC system
P_{fc}	FC-side output power
P_{pv}	PV-side output power
THD	Total harmonic distortion
V_{dc}	DC-link voltage
V_{fc}	FC voltage
V_{pv}	PV voltage

In a normal condition, grid currents and power flows are balanced at the grid-side. For this, the electrical system is fundamentally symmetrical, and hence positive-sequence currents only seem in an electrical line. But, unbalanced loads distorts the equilibrium of grid currents, which are in the ratings of different magnitudes [15]. These components also distort the power balance supplied to the grid-side, thereby triggering the system losses and reducing the running efficiency [16]. And this condition creates negative & zero sequence components at grid-side currents. For this purpose, the elimination of negative & zero sequence currents at the grid-side is an essential issue for unbalanced load conditions. Thus, an improved power flow controller is proposed in this study to provide stability at grid-side currents. In this way, the proposed method controls the power equilibrium at grid-side power flows to eliminate unwanted sequence components.

1.2. A brief review

In grid-connected hybrid energy systems, energy generation units such as PVs, FCs, batteries and/or super-capacitors generate electrical power in dc-form [8]. However, it is common knowledge that the electrical power in dc form must be converted into ac-form for the grid interconnection [17]. In order to provide a smooth connection, these generation units are linked to utility-grids by using electrical interface components [18]. In a conventional system, the fundamental components are dc-dc converter and inverter, and power flow management is provided through inverter elements [19,20]. The input inverter is connected with a dc-dc converter, which provides a smooth voltage within an optimum control [21]. For this, the significant control of a grid-connected PV/FC system is achieved based on pulse-width modulated inverters. The main target of inverters is to supply active power from energy generation units to loads/utilities and control the supplied currents/dc-link voltage [22]. There are many studies related to energy management used in grid-connected hybrid energy systems in the literature. The common function of these studies is to control power flow between grid and energy units. A lot of studies are considered for three-phase balanced sensitive loads in Refs. [17,19–22]. In these studies, it takes attention to power flow control with optimization approaches. But, these works are tested under balanced loading situations.

Considering the existing studies, the system structures in Refs [23,24] are considered for on-grid and off-grid modes with three-phase balanced sensitive loads. In Ref. [25], the system is performed under unbalanced grid fault situations. However, only negative sequence components are compensated through a positive–negative sequence extraction method. In Refs. [26,27], the fundamental subject is the compensation of current harmonics under three-phase balanced nonlinear loads. Also, a hybrid system with reactive loads is analyzed in Ref. [28]. Besides, Ref. [29,30], Ref. [31], and Ref. [32] are interested in single-phase systems for sensitive loads, nonlinear loads, and no-load conditions, respectively. These studies are not analyzed for unbalanced loading conditions. In Ref, [33], zero-sequence components are only compensated at the grid-side. In Ref. [34], the system is performed under no load with unbalanced grid fault conditions, which cause unbalanced currents. In this study, the positive–negative sequence method is implemented with a three-phase three-wire inverter to provide balanced currents. Ref. [35] uses a droop controller to provide system stability under unbalanced grid situations. The common point of these methods in Refs. [34,35] is that the systems are tested under unbalanced grid-conditions and based on three-phase three-wire inverters. This condition makes them applicable to the compensation of only negative sequence components. For this purpose, in this study, an improved power flow control method is proposed to compensate negative and zero sequence components at the grid-side. Also, the system is tested under unbalanced loads balanced grid voltages in contrast to classical systems. By this way, the compensation of zero-sequence currents at grid-side is aimed in addition to negative sequence components in this study.

1.3. Key contributions

In comparison with traditional grid-interfaced hybrid renewable energy systems, the current study introduces a grid-side phase balancing method with negative/sequence current elimination. To eliminate the negative&zero sequence current, the proposed energy management scheme is based on αβ/dq transform instead of conventional abc/dq transform. Thus, the proposed method needs more voltage/current measurements compared to conventional abc/dq method. This makes the proposed method more complicated and difficult in comparison with the conventional energy management method. But, the proposed energy management scheme ensures that the grid-connected hybrid energy system operates more stable under unbalanced loading conditions. This mitigation may play a significant role to (1) increase the efficiency, (2) increase the system relaiblity, (3) reduce the power system losses, and (4) prevent the malfunction of the overall system.

In the current study, an energy management scheme is developed to supervise power flow control between energy units amd grids/loads. The applicability of the proposed scheme is designed and tested in a grid-interfaced PV/FC hybrid energy system under unbalanced loading condition. In order to show the validity of the developed energy management scheme, different case studies are further presented in comparison with conventional power flow control strategy. Regarding the comparison results, the overall system has been built and tested using Simulink environment program.

In this paper, a grid-connected PV/FC hybrid energy system is designed and performed for unbalanced load & balanced grid voltage conditions. The unbalanced loading situations distorts the grid-current stability and cause unbalanced currents at grid-side. To obtain balanced grid-currents under unbalanced loading situations, the elimination of negative&zero sequence current are proposed in this study. To this end, the grid-connected hybrid energy system is controlled through the proposed phase balancing method to ensure grid stability. The operating principles of the proposed control method are also detailed in the study. Moreover, the main objectives of the study are given as follows:

- In the designed system, hybrid-energy system unit supplies more power to the phase where the load consumes higher power. Also, it supplies less power to the phase where the load consumes less power. In this regard, the controller provides power balancing at the grid-side. This also means that the grid-side currents under constant voltage are balanced.
- In order to control each phase separately, the system uses H-bridge inverters. For this, multiple frame αβ/dq conversion with the power differentiation part is used for each grid inverter.
- With the power balancing, the negative and zero sequence components due to unbalanced loading situations are eliminated at grid-side currents. The numerical values show the validity of the proposed method in comparison with the conventional power flow control strategy.

The paper organization is as follows: Firstly, the structure of the designed system is introduced in part 2. Subsequently, the phase balancing method is presented in detail in part 3. In this part, the control is explained through algorithm, scheme, and mathematical expressions. In part 4, performance results are introduced to verify the proposed control method's effectiveness compared to the conventional power flow method. Then, a brief conclusion is also given in part 5.

2. Hybrid system with phase balancing method

A grid-connected hybrid energy system a dual-input boost converter, an inverter, ripple filter and transformer (optional). Among interface elements, dc-dc converter and inverter are the main components that control the power flow from the FC to the grid. Dc-dc converter generally increases dc voltage and stabilized the dc voltage at output [36]. Dc voltage at the dc-dc converter's output is converted to ac form through inverter elements [37]. In this way, the inverter converts the dc-link voltage into a controlled ac form. Switching ripple filter connected to the inverter is used to reduce the unwanted components at the inverter output [38,39]. The transformer is optional, and its function is to integrate with high voltage electrical lines [33].

In designed hybrid energy topology, it consists of PV and FC energy units, as shown in Fig. 1. The system is connected to unbalanced sensitive (resistive) loads under balanced grid voltages. It is also constructed by using H-bridge inverters and connected to the grid through three single-phase isolation transformers. The system proposes to control each phase separately through the presented control strategy.

2.1. Energy generation units

This part presents the system elements employed in the hybrid energy system. The energy generation units are PV and FC in the power ratings of 15.6 kW and 19.3 kW.

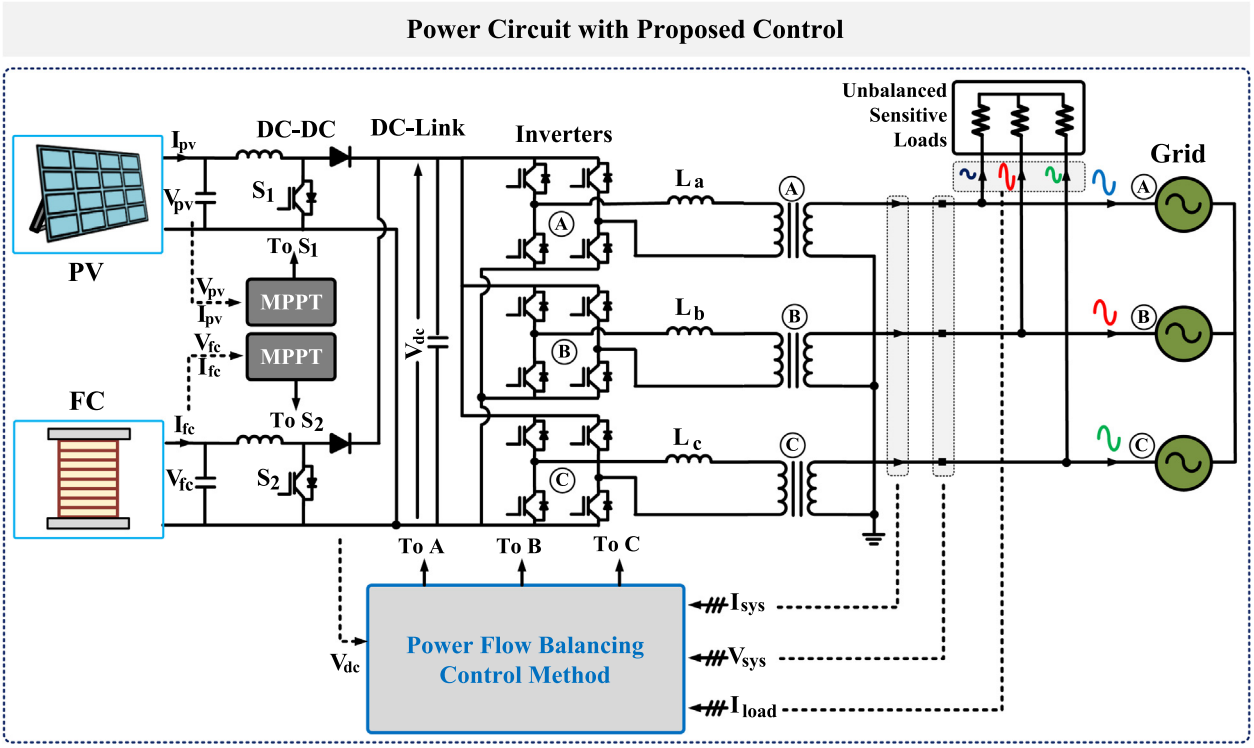

Fig. 1. The power circuit with phase balancing method.

2.1.1. PV

PV panel generates dc electrical energy through solar rays [40], and its output power depends on the different variables such as irradiance, temperature, and solar cell characteristics [41,42]. The output power of the PV unit (P_{pv}) is described below [33]:

$$P_{pv} = (N_s \times N_p) P_{nom} \left(\frac{G}{G_{nom}}\right) \left[1 + \alpha \left(T_{c,actual} - T_{nom}\right)\right] \quad (1)$$

N_s and N_p express the series and parallel PV modules. P_{nom} is power value in the optimum operating. G indicates irradiance value, and G_{nom} defined irradiance value at 1000 W/m^2 .$T_{c,actual}$ is the temperature value of PV array, and T_{nom} is nominal temperature. Also, α defines a fixed temperature parameter [43,44].

The output current in a PV cell is defined as [40]:

$$I_{sc} = I_{ph}(1 + C_o(T - 273)) - I_o\left(e^{\frac{q(V_{pv}+I_{sc}R_s)}{nkT}} - 1\right) - \frac{V_{pv} + I_{sc}R_s}{R_{sh}} \quad (2)$$

2.1.2. FC

Proton exchange membrane FCs (PEMFC) are used as the second energy generation input of hybrid energy system. Its dynamic response is defined in Eqs. (3)–(6). The operating voltage of FC is computed as [45]:

$$V_{fc} = V_{oc} - V_{ohmic} - v_d \quad (3)$$

V_{fc} is the output voltage of FC stack, V_{oc} is the open-circuit voltage and V_{ohmic} defines the loss voltage. Besides, v_d expresses the absolute polarization overvoltage, which is defined by using .. and I_{fc}[46,47]. Open circuit voltage (V_{oc}) is formulated as:

$$V_{oc} = K_c\left[V_o + (T - 298)\frac{-44,43}{zF} + \frac{RT}{zF}\ln\left(\frac{P_{H_2}P_{O_2}^{1/2}}{P_{H_2O}}\right)\right] \quad (4)$$

V_o is an electromotive force for constant pressure. and z is electron value [48]. Loss voltage (V_{ohmic}) is defined according to internal resistance and FC current [49].

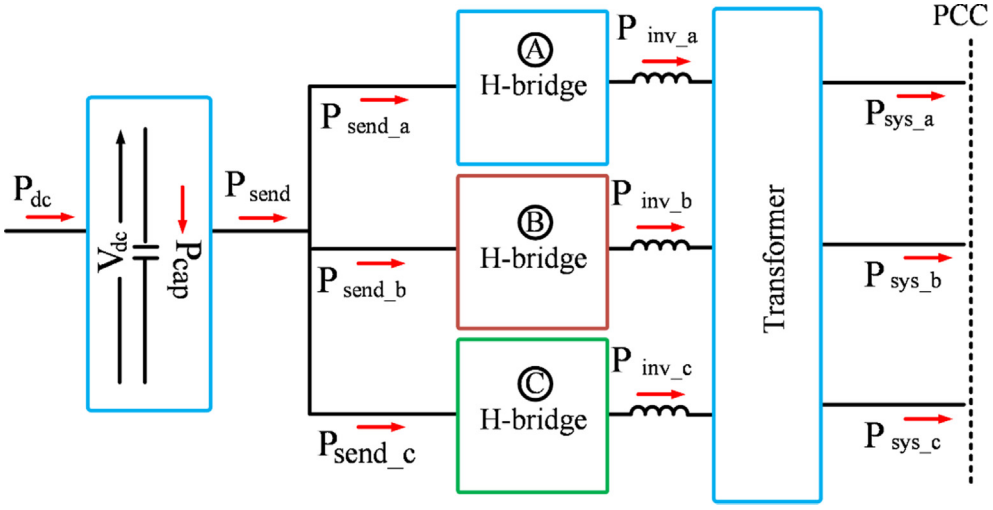

Fig. 2. The power exchange through separate inverters.

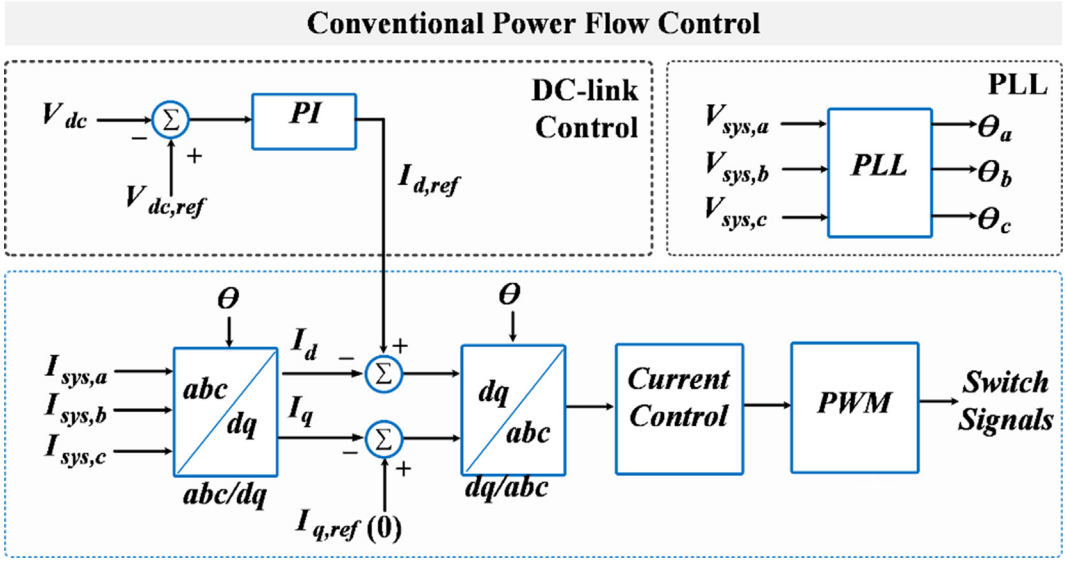

Fig. 3. Conventional power flow controller for grid inverters.

$$V_{ohmic} = i_{fc} R_{ohmic} \tag{5}$$

Polarization overvoltage (v_d) is also defined as:

$$V_d = N \times A \times \ln(i_{fc}/i_o) \tag{6}$$

N indicates the cells in the FC. A and i_o are Tafel slope and exchange current given in [48].

2.2. Interface elements

Among interface elements, dc-dc converters provide a fixed input voltage for the inverter unit [32,36]. In the designed system, dual input single output dc-dc boost converter is used to keep and stabilize the dc-link voltage. The relationship between input and output voltage is defined in Eq. (7).

$$V_{dc} = \begin{Bmatrix} V_{fc}/(1 - D_{fc}) & for \quad FC \\ V_{pv}/(1 - D_{pv}) & for \quad PV \end{Bmatrix} \tag{7}$$

D_{pv} and D_{fc} are switching ratios of S1 and S2 in dual input boost converter.

In the control section of boost converter, perturb and observe maximum power point tracking method (P&O MPPT) is employed to generate switching signals for S1 and S2. Online iterative method P&O MPPT generates a reference duty cycle value and determines the voltage conversion ratio through the duty cycle. In the operational process, MPPT is operated via observation for positive and negative alteration values of PV/FC units [41].

$$\begin{Bmatrix} \frac{dV_{in}}{dt} = \frac{1}{C_{in}}(i_{inductor} - i_{in}) \\ \frac{di_{inductor}}{dt} = \frac{1}{L_{boost}}(D-1)V_{in} - \frac{R_{boost}}{L_{boost}} i_{inductor} \end{Bmatrix} \tag{8}$$

In the boost converter, the switching of the dual input boost converter is accomplished at 5 kHz in order to keep dc-link voltage constant at 150 V. Also, the value of the inductor is selected as 0.5 mH by using $L_{boost} = V_{in}D/(\Delta i_{inductor} f)$.

Fig. 2 presents the power flow circuit in the H-bridge inverters based system. It shows that the sending power (P_{send}) is supplied to the grid-side through separate inverters. The primary function of inverters is to supply controlled power for each phase at calculated values.

The power value at the dc-link point is defined below [50,51].

$$P_{dc} = P_{cap} + P_{send} \tag{9}$$

P_{dc} and P_{cap} are coming energy and stored energy, respectively. P_{send} defines sent power through inverters. The relationship in sending powers is written for three phases:

$$P_{send} = P_{send\_a} + P_{send\_b} + P_{send\_c} \tag{10}$$

$$P_{sys} = P_{sys\_a} + P_{sys\_b} + P_{sys\_c} \tag{11}$$

P_{sys} is defined as supplied power from the system to the point of common coupling. If we neglect the power losses due to the inverter and transformer, the sending power is approximately identical to the system power, described in Eq. (12).

$$P_{send} \approx P_{inv} \approx P_{sys} \tag{12}$$

Readjusting the Eq. (9), it is written in a new form:

$$P_{dc} = P_{cap} + P_{sys} \tag{13}$$

Due to $P_{cap} = V_{dc} C_{dc} \frac{dV_{dc}}{dt}$, the relationship between P_{dc} and P_{sys} is described below:

$$P_{dc} = P_{sys} + V_{dc} C_{dc} \frac{dV_{dc}}{dt} = P_{sys} + V_{dc} C_{dc} \frac{\Delta V_{dc}}{\Delta t} \tag{14}$$

We assume that P_{dc} has no active power. In this way, the dc-link voltage changes linearly with the system power. Thus, the voltage change in Eq. (14) is rewritten, as given in Eq. (15).

$$\frac{\Delta V_{dc}}{\Delta t} = \frac{-Psys}{V_{dc} C_{dc}} \tag{15}$$

3. Phase balancing method

The proper power flow control from energy generation units to utility-grids/loads is provided through inverter operation. The supplied ac power is synchronized through the inverter part and efficiently transferred into the utility-grids by the power flow controller. For the proper operation, the grid inverter should provide (1) the grid synchronization and unity power factor, (2) control of active/reactive power, (3) supervising of dc-link voltage control, and (4) balancing the power flow at all phases.

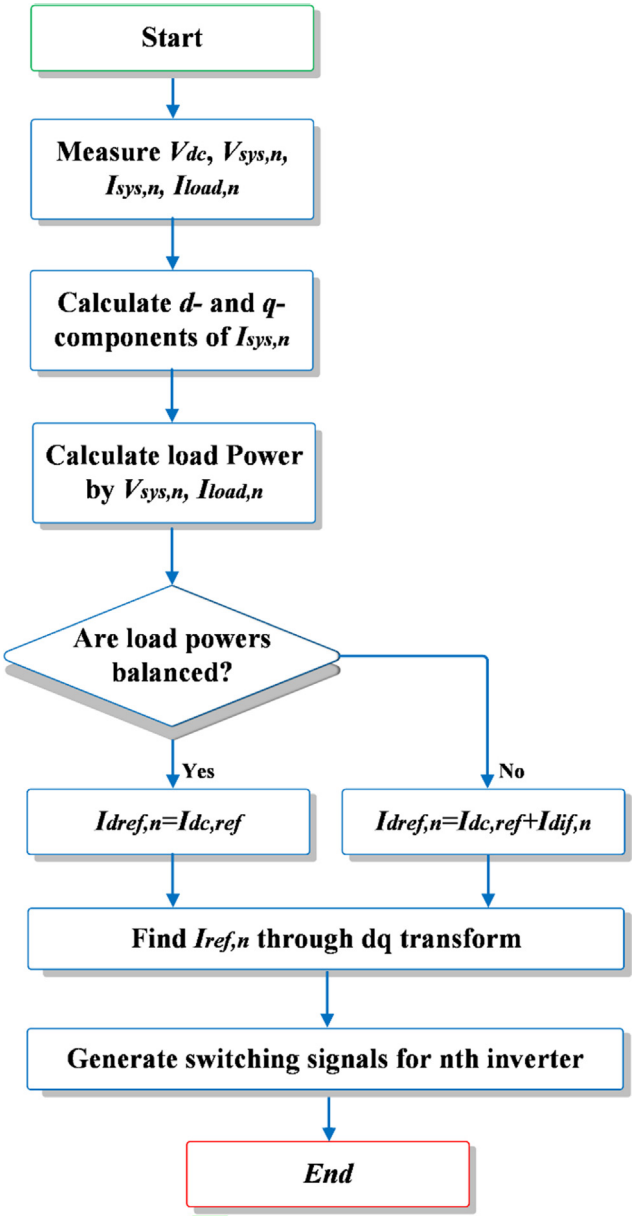

Fig. 4. Flowchart of the phase balancing method for the designed system.

3.1. Conventional power flow method

Fig. 3 shows the structure of a conventional power flow control strategy implemented in grid inverters. According to the controller scheme, it is designed to provide the stabilization of active/reactive power for balanced three-phase systems. In the grid interconnection, dq based control theory is used by using actual/reference values of system currents. But, this structure is not robust and stable under unbalanced current conditions. Because, the power flow controller generates symmetrical reference values by using abc/dq transform, thereby supplying balanced powers from the system. This situation makes the controller cannot be applied for unbalanced grid/load conditions.

3.2. Proposed algorithm

The proposed power flow control algorithm is presented through a flowchart, as shown in Fig. 4. The proposed phase balancing method can be summarized as follows.

Step 1: Measure the dc-link voltage (V_{dc}), system voltages ($V_{sys,n}$), system currents ($I_{sys,n}$) and load currents ($I_{load,n}$). In definitions, n indicates phases a, b, c.
Step 2: Generate orthogonal signals of system currents for each phase. Then, Calculate d- and q- components for each phase current (I_{dn}),
Step 3: Calculate load powers by using system voltages ($V_{sys,n}$) and load currents ($I_{load,n}$). If load powers are unbalanced, calculate the differentiation value to stabilize grid powers and add the differentiation value (a current reference ($I_{dif,n}$)) to the current reference value ($I_{dc,ref}$)) generated through dc-link voltage. If load powers are balanced, the reference current of d-component is equal to $I_{dc,ref}$.
Step 4: In the next process, find reference values ($I_{ref,n}$) through dq/αβ transform. In this step, α- components are used as reference according to the separate-phase structure.
Step 5. The final step is the generation of switching signals to provide power flow control from the hybrid energy system to the grid.

3.3. Proposed control scheme and reference generation

The proposed method's control scheme is used in the H-bridge inverter-based PV/FC energy generation system with unbalanced sensitive loads. Compared with the conventional method, it adjusts the controlled power flow for each phase at different amounts. The main function of control is to supply more power to the phase where the load consumes higher power, and supply less power to the phase where the load consumes less power. In this way, the controller provides power balancing at the grid-side. By this way, the negative/zero sequence components are eliminated at grid-side currents thanks to the power flow balancing. Fig. 5 shows the proposed control method implemented in the designed system. The scheme shows that active power is controlled by using d component, which is calculated by using (I_{dn}), ($I_{dif,n}$) and ($I_{dc,ref}$).

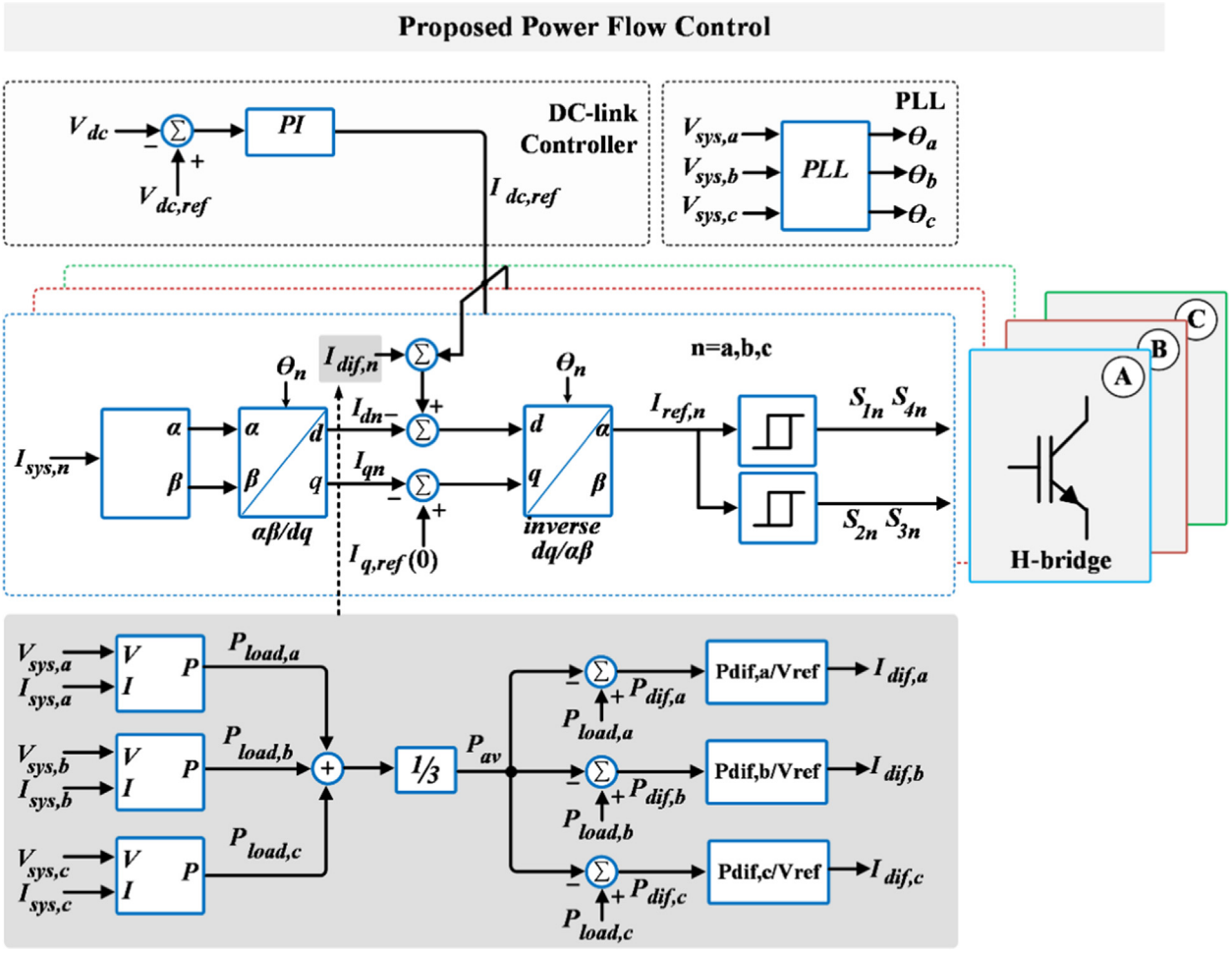

Fig. 5. The proposed scheme: phase balancing method.

Reactive power is controlled through q-components of system currents, and reference value $I_{q,ref}$ is equal to zero [52].

For a three-phase system, the supplied powers are computed through system voltages and system currents [53]. The power magnitudes in dq frame are written as:

$$P_{sys,n} = \frac{3}{2}\left(V_{sys,n-d} i_{sys,n-d} + V_{sys,n-q} i_{sys,n-q}\right) \quad (16)$$

$$Q_{sys,n} = \frac{3}{2}\left(V_{sys,n-q} i_{sys,n-d} - V_{sys,n-d} i_{sys,n-q}\right) \quad (17)$$

In the equations, it is clear that active/reactive power values are calculated using d- and q- components of system currents [54]. If the system voltage is oriented as d-component, the d- and q- voltages are defined as:

$$V_{sys,n-d} = V_{sys,n} \quad (18)$$

$$V_{sys,n-q} = 0 \quad (19)$$

Arranging the Eq. (16) and Eq. (17), the powers are rewritten in Eq. (20) and Eq. (21) [53,54]:

$$P_{sys,n} = \frac{3}{2} V_{sys,n-d} i_{sys,n-d} \quad (20)$$

$$Q_{sys,n} = -\frac{3}{2} V_{sys,n-d} i_{sys,n-q} \quad (21)$$

Dc-link voltage is used to control the active power supply. For this, the reference value of dc-link t is written as:

$$I_{dc,ref} = K_p(V_{dc,ref} - V_{dc}) + K_i \int (V_{dc,ref} - V_{dc})dt \quad (22)$$

For no reactive power supply, the reference value of the q-component must be zero.

$$I_{q,ref} = 0 \quad (23)$$

D- and q- components of system currents are calculated by using α- and β- components of system currents.

$$\begin{bmatrix} I_{dn} \\ I_{qn} \end{bmatrix} = \begin{bmatrix} \cos(\omega t) & \sin(\omega t) \\ -\sin(\omega t) & \cos(\omega t) \end{bmatrix} \begin{bmatrix} I_{sys,n-\alpha} \\ I_{sys,n-\beta} \end{bmatrix} \quad (24)$$

According to the αβ/dq transformation, I_{dn} and I_{qn} components are defined below:

Table 1
System parameters.

Parameter	Value	Unit	Parameter	Value	Unit
DC-DC Converter			**STX Solar STX-250MT2**		
Type	DISO Boost	[–]	Parallel strings	26	[–]
Inductances (L_1, L_2)	1	[mH]	Series modules in a string	3	[–]
Capacitance (Cdc)	10 mF	[mF]	Maximum power	250.1	[W]
Switching	5	[kHz]	Cells in a module	60	[–]
Inverter			Open circuit voltage	38.19	[V]
Type	H-bridge	[–]	Short circuit current	8.8	[A]
Filter inductance	1	[mH]	Voltage at max. power	30.5	[W]
Transformer	15*3	[kVA]	Current at max. power	8.2	[A]
Grid			**Ballard PEMFC 9SSL**		
Voltage (Phase rms)	220	[V]	Number of cell	110	[–]
Frequency	50	[Hz]	Voltage at 0 A and 1 A	[106.15,104.61]	[V,V]
Resistive Loads			Nominal operating point	[260,73.4]	[A,V]
[Ra,Rb,Rc]	[12,8,10]	[ohm]	Maximum Operation values	[320,64]	[A,V]

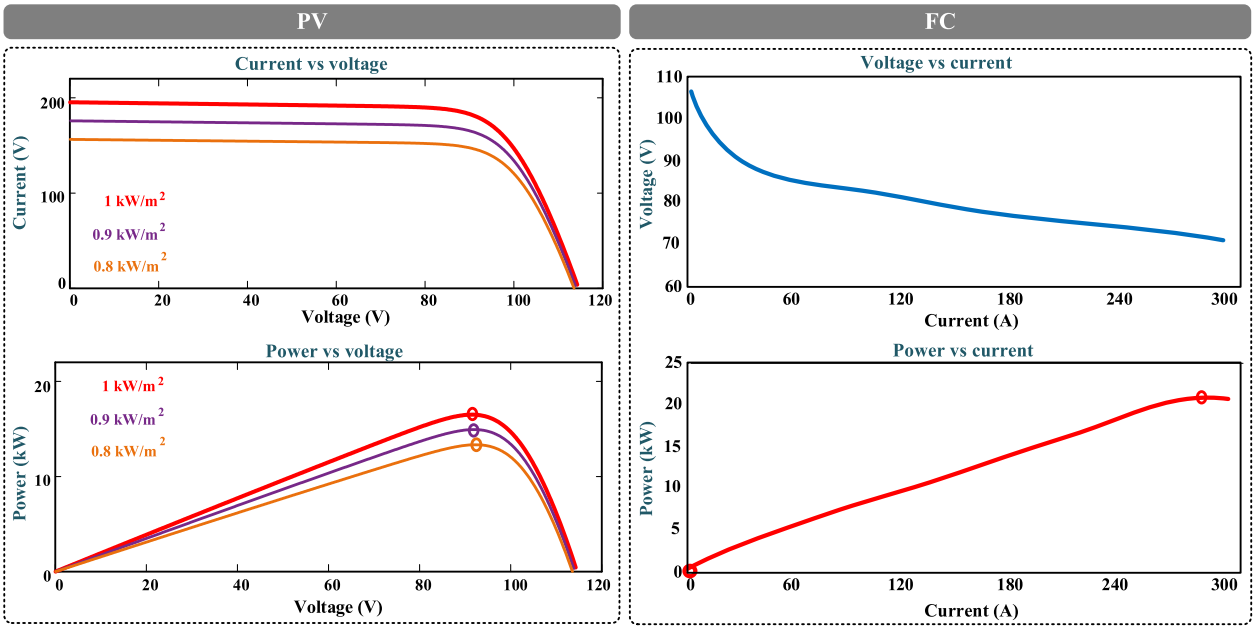

Fig. 6. The electrical characteristics of STX Solar STX-250MT2 PV Panel and Ballard FC-Velocity 9SSL PEMFC.

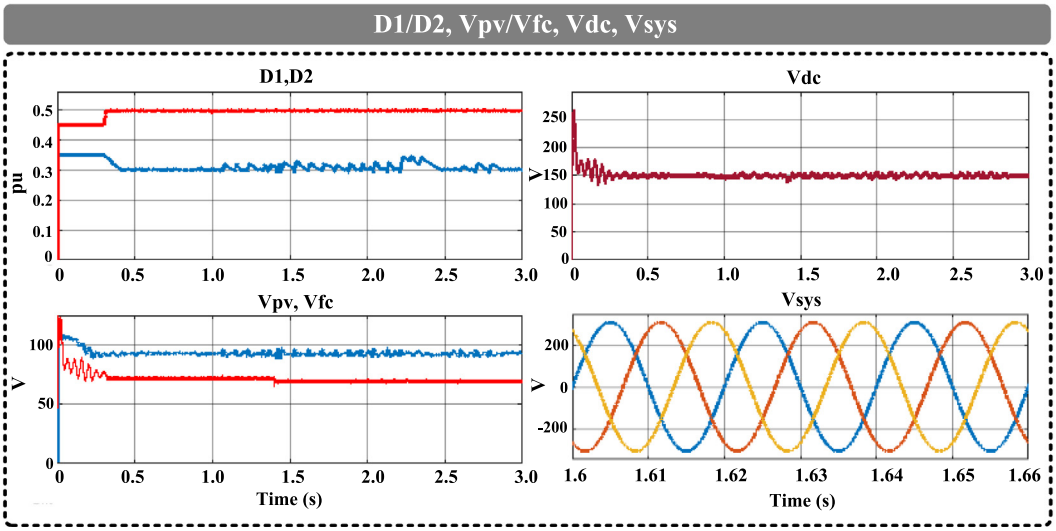

Fig. 7. The waveforms of duty cycles (for S1 and S2), input PV/FC voltages, dc-link voltage, and system voltages.

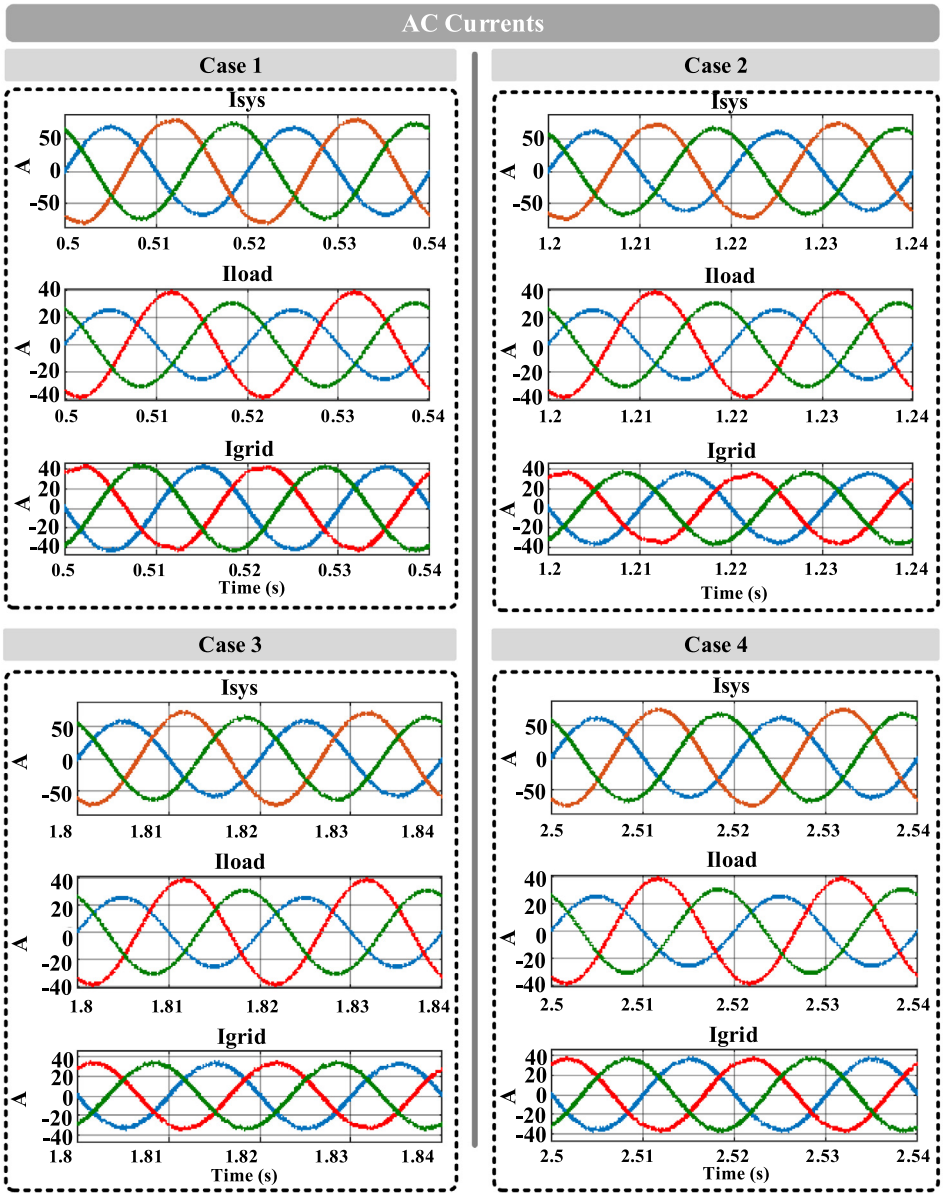

Fig. 8. System currents at point of common coupling for state 1, state 2, state 3, and state 4.

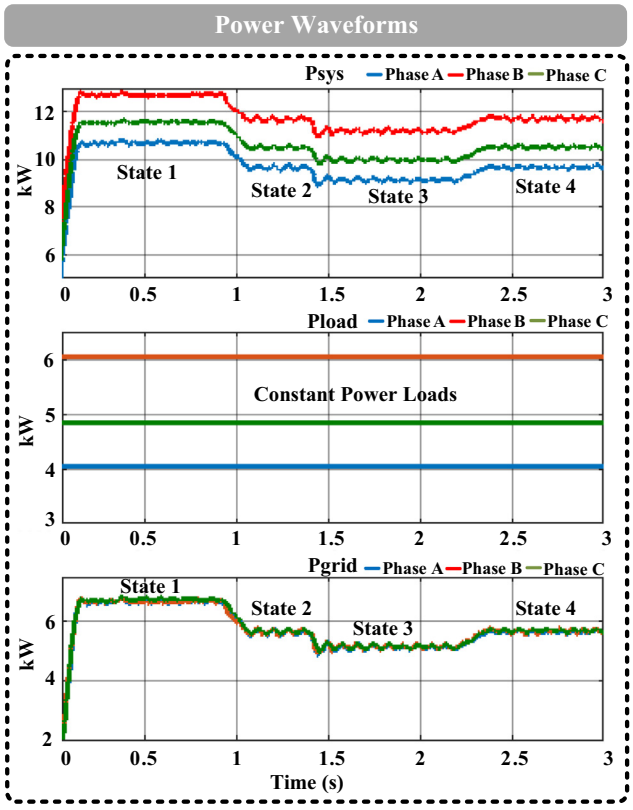

Fig. 9. Power flows in grid-connected PV/FC system with phase balancing method.

$$I_{dn} = I_{sys,n-\alpha}\cos(\omega t) + I_{sys,n-\beta}\sin(\omega t) \tag{25}$$

$$I_{qn} = -I_{sys,n-\alpha}\sin(\omega t) + I_{sys,n-\beta}\cos(\omega t) \tag{26}$$

In order to provide power balancing at the grid-side, load powers are calculated. In the case of an unbalanced condition, the reference differentiation values are added into $I_{dc,ref}$. This process increases or decreased the supplied active power from each phase in a controlled way. The power values of sensitive loads are:

$$P_{load,n} = V_{sys,n} I_{sys,n}\cos\theta_n \tag{27}$$

In the next step, the average value of load power is calculated:

$$P_{av} = \frac{1}{3}\sum_{n=1}^{3} P_{load,n} \tag{28}$$

The calculated average value is subtracted from each phase value to find each phase's differentiation power value. This step is realized as follows:

$$\left\{\begin{array}{l} P_{dif,a} = P_{load,a} - P_{av} \\ P_{dif,b} = P_{load,b} - P_{av} \\ P_{dif,c} = P_{load,c} - P_{av} \end{array}\right\} \tag{29}$$

The differentiation values which will be added to the d-component, are calculated by using current control.

$$I_{dif,n} = K.P_{dif,a} \tag{30}$$

After that, the d and q components as a difference are given in Eqs. (29–30). These components are named error currents in dq frame.

$$I_{derror,n} = I_{d,ref} + I_{dif,n} - I_{dn} \quad n = a,b,c \tag{31}$$

$$I_{qerror,n} = I_{q,ref} - I_{qn} = -I_{qn} \quad n = a,b,c \tag{32}$$

The obtained d- and q components of error are used to generate reference currents, which is used to trigger switching signals through the current controller PWM. For this, the d- and q- components are converted into α components through dq/αβ transform.

$$\left\{\begin{array}{l} I_{ref,a} = I_{derror,a}\cos\theta_a + I_{qerror,a}\sin\theta_a \\ I_{ref,b} = I_{derror,b}\cos\theta_a + I_{qerror,b}\sin\theta_a \\ I_{ref,c} = I_{derror,c}\cos\theta_a + I_{qerror,c}\sin\theta_a \end{array}\right\} \tag{33}$$

Finally, the reference current values ($I_{ref,n}$) are employed to generate switching signals ($S_{1n}, S_{2n}, S_{3n}, S_{4n}$) through hysteresis current control. The switching rules of current control are defined in Eq. (34).

$$\textit{Switching States} = \left\{\begin{array}{ll} I_{ref,a} > +h & S_{1a}, S_{4a} \\ I_{ref,a} < -h & S_{2a}, S_{3a} \\ I_{ref,b} > +h & S_{1b}, S_{4b} \\ I_{ref,b} < -h & S_{2b}, S_{3b} \\ I_{ref,c} > +h & S_{1c}, S_{4c} \\ I_{ref,c} < -h & S_{2c}, S_{3c} \end{array}\right\} \tag{34}$$

In the switching process, the hysteresis band values (+h and -h) for the control method are 0.02 and −0.02. In this process, reference signals produced for each phase are compared with hysteresis band values. If the reference signal is higher than + h band, S_{1n}, S_{4n} signals are produced. The switches (S_{1n}, S_{4n}) will remain in the conduction state until the produced reference signal decreases to −h. When the reference signal drops below the value of −h, the switches (S_{2n}, S_{3n}) will go into the conduction state, while the switches in

Table 2
Power values for three-phase and four states.

	PV/FC Operation		Power Flow Values		
	PV	FC	From System	To Load	To Grid
Case 1	1000 W/m^2	328 Kelvin	PhA: 10.75 kW	PhA: 4.03 kW	PhA: 6.72 kW
			PhB: 12.71 kW	PhB: 6.04 kW	PhB: 6.67 kW
			PhC: 11.58 kW	PhC: 4.83 kW	PhC: 6.75 kW
Case 2	800 W/m^2	328 Kelvin	PhA: 9.54 kW	PhA: 4.03 kW	PhA: 5.51 kW
			PhB: 11.79 kW	PhB: 6.04 kW	PhB: 5.75 kW
			PhC: 10.48 kW	PhC: 4.83 kW	PhC: 5.65 kW
Case 3	800 W/m^2	320 Kelvin	PhA: 9.12 kW	PhA: 4.03 kW	PhA: 5.09 kW
			PhB: 11.18 kW	PhB: 6.04 kW	PhB: 5.14 kW
			PhC: 9.85 kW	PhC: 4.83 kW	PhC: 5.02 kW
Case 4	900 W/m^2	320 Kelvin	PhA: 9.654 kW	PhA: 4.03 kW	PhA: 5.62 kW
			PhB: 11.69 kW	PhB: 6.04 kW	PhB: 5.65 kW
			PhC: 10.57 kW	PhC: 4.83 kW	PhC: 5.74 kW

the conduction state will be in the cut-off state. The switches will remain in the conduction mode until the reference signal reaches + h. In these explanations, n indicates the phases a, b and c.

4. Performance results

The complete grid-connected PV/FC model is used to test the proposed control scheme using Matlab/Simulink environment program. Also, the performance results are compared with the conventional power flow method in order to show the validity of the proposed control scheme. The parameter values of the grid-connected hybrid energy system are introduced in Table 1. In the system, STX Solar STX-250MT2 PV panels are performed to produce 16.5 kW in output power ratings. At this operating point, voltage/current values are defined as 24.5 V/8.16 A for maximum power. Ballard FCvelocity 9SSL PEMFC is the second energy generation input of the hybrid system. The maximum power of PEMFC is 19.3 kW in the rating of 73.4 V, 260 A.

Fig. 6 shows the electrical characteristic waveforms of the PV panel and FC stack. For nominal value (1000 W/m2, 25 °C), 15.6 kW power is extracted at 91.5 V/170 A from PV. The FC can generate approximately 19.3 kW for nominal operation.

The modeled system is tested for different case studies. The case studies are defined as follows:

- Case 1: operating at 1000 W/m^2 and 328 Kelvin for PV and PEMFC, respectively
- Case 2: operating at 800 W/m^2 and 328 Kelvin for PV and PEMFC, respectively

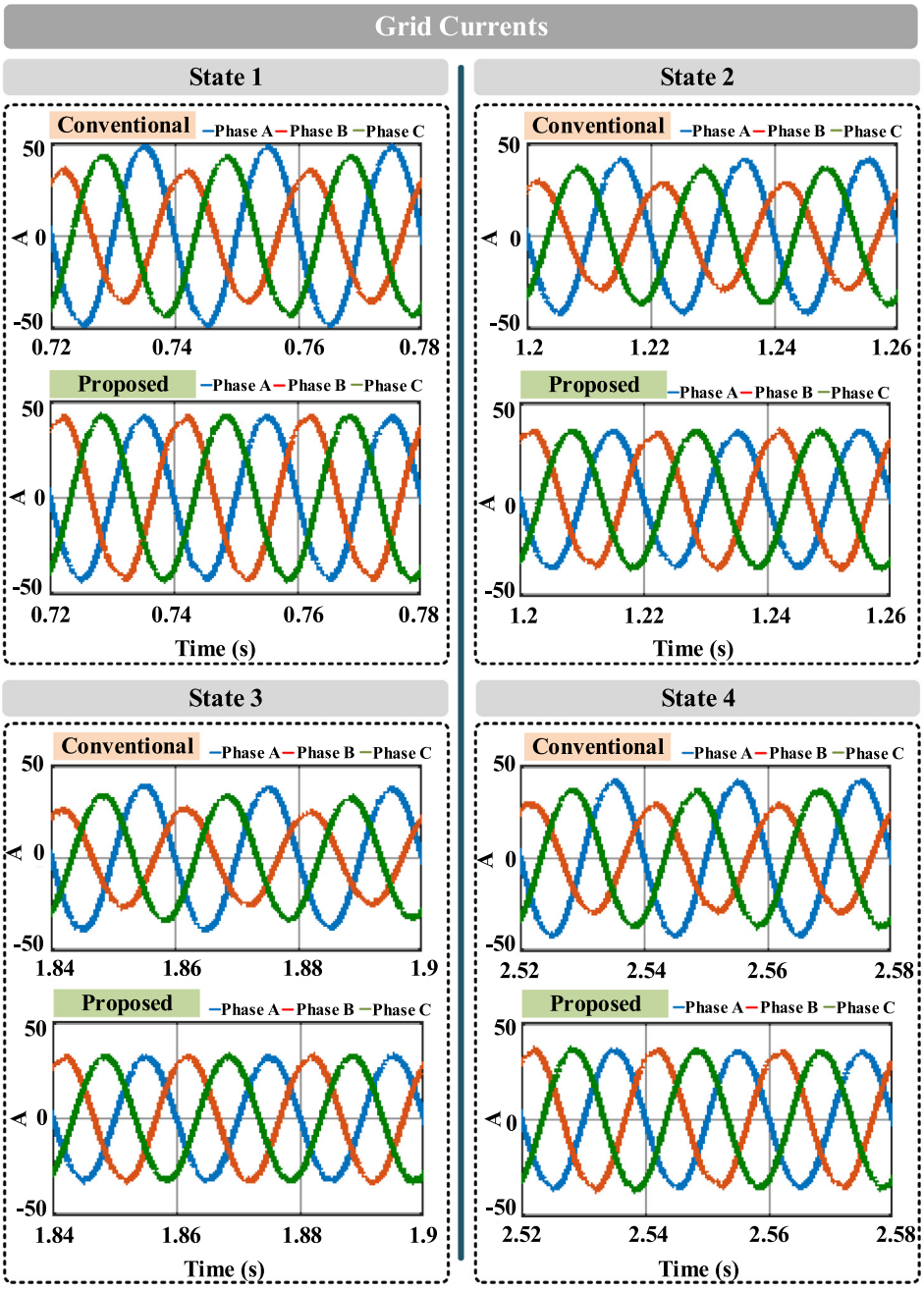

Fig. 10. The grid currents according to conventional/proposed method based system.

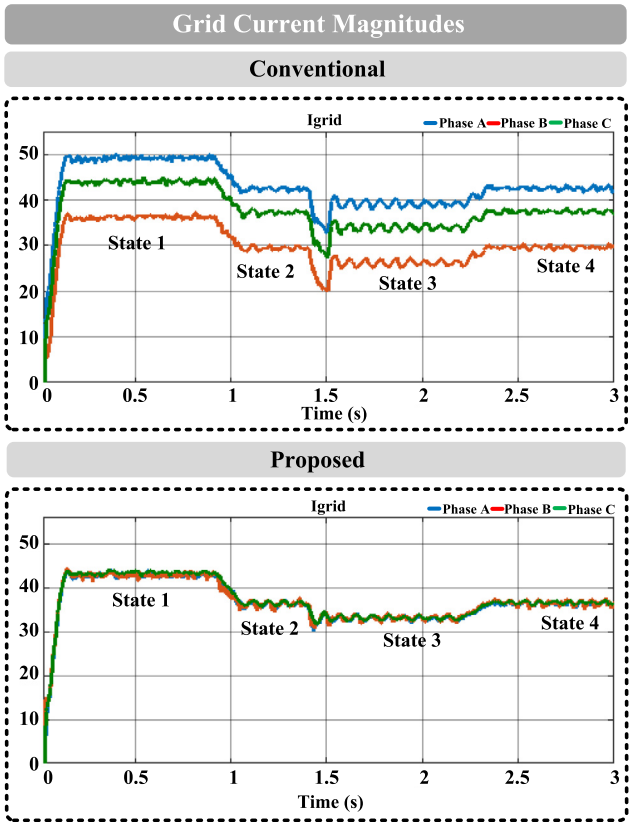

Fig. 11. The magnitudes of grid-currents for three states through conventional/proposed systems.

- Case 3: operating at 800 W/m^2 and 320 Kelvin for PV and PEMFC, respectively
- Case 4: operating at 900 W/m^2 and 320 Kelvin for PV and PEMFC, respectively

The waveforms of duty cycles (D1 and D2), PV/FC voltages (Vpv and Vfc), dc-link voltage (Vdc) and system voltages are presented in Fig. 7. Performance results show that MPPTs generate different duty cycles to keep the dc-link voltage constant according to input PV/FC voltages. The dc-link capacitor's voltage is kept at 150 V. PV generates approximately 93 V at the output-side. However, FC operates at 72 V for 328 Kelvin and at 68 V for 320 Kelvin. The system voltage is balanced, stable, and identical to grid voltages. The peak values of system voltages are 311 V.

The system currents in ac form are given in Fig. 8. It shows system current, load currents, and grid currents for four states. As shown in waveforms, the loads draw unbalanced currents according to the resistive load values. Therefore, the system supplies the active power and supplies currents in a controlled manner. As a result, the magnitudes of grid currents are equal to each other for all phases.

The power flow waveforms of grid-connected PV/FC system with phase balancing method are introduced in Fig. 9. The consumed powers by loads are constant, and their values are different. The load powers are 4.03 kW, 6.04 kW, 4.83 kW for phase a, phase b, and phase c. The system generated active power and supply to grid/loads according to the condition. The power values at the grid-side are nearly kept at a constant value, as shown in waveforms. The detailed results for power values for four states are given in Table 2.

The main function of the proposed method is to provide balanced currents at the grid-side through power balancing. In this

Table 3
The magnitudes of grid-currents for conventional/proposed method based systems.

	Grid Currents					
	Conventional			Proposed		
	Phase A	Phase B	Phase C	Phase A	Phase B	Phase C
Case 1	48.8 A	43.9 A	35.7 A	42.7 A	42.9 A	43.4 A
Case 2	43.2 A	37.1 A	28.8 A	35.8 A	35.6 A	35.8 A
Case 3	39.8 A	34.2 A	27.2 A	32.2 A	32.6 A	32.7 A
Case 4	43.4 A	36.8 A	28.8 A	36.5 A	36.9 A	36.8 A

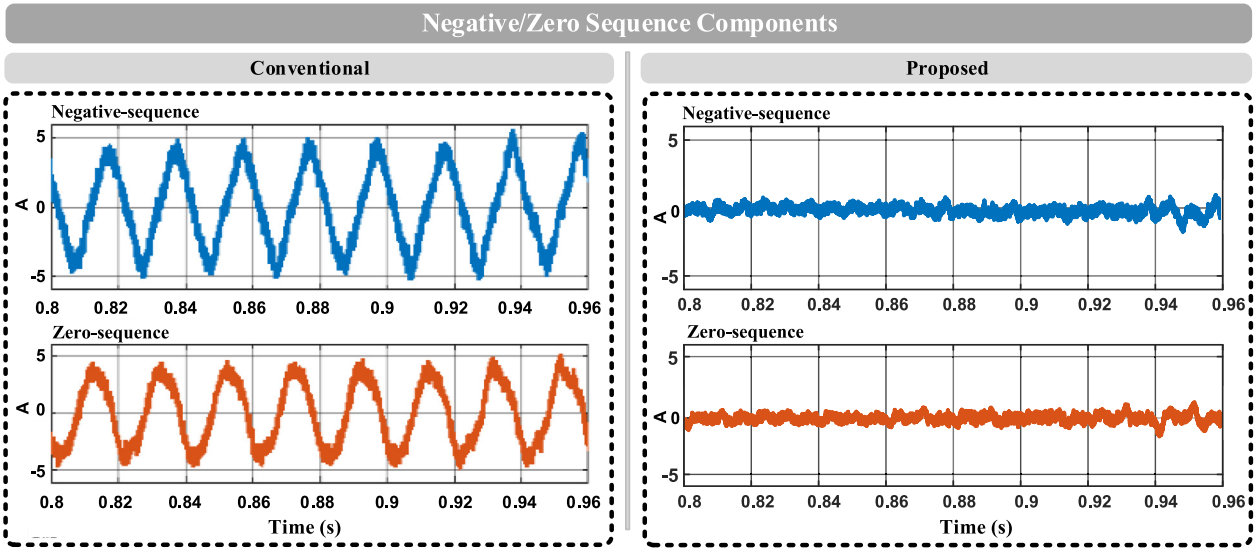

Fig. 12. The waveforms of negative/zero-sequence components for conventional/proposed method.

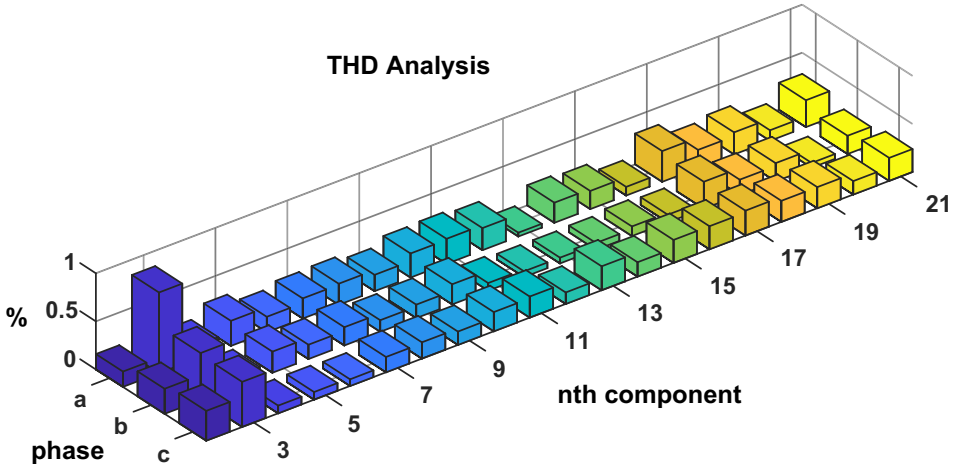

Fig. 13. THD analysis of grid currents up to 21th harmonics.

Table 4
The percentage values of harmonic components of grid-side currents.

Order	Phase			Order	Phase		
	Phase A	Phase B	Phase C		Phase A	Phase B	Phase C
2nd	0.12	0.18	0.21	**12th**	0.28	0.09	0.22
3rd	0.91	0.84	0.87	**13th**	0.05	0.11	0.37
4th	0.09	0.08	0.06	**14th**	0.29	0.12	0.24
5th	0.32	0.29	0.16	**15th**	0.26	0.15	0.41
6th	0.27	0.26	0.19	**16th**	0.18	0.21	0.44
7th	0.26	0.27	0.28	**17th**	0.45	0.44	0.44
8th	0.29	0.24	0.30	**18th**	0.28	0.31	0.32
9th	0.21	0.24	0.27	**19th**	0.29	0.29	0.32
10th	0.27	0.26	0.29	**20th**	0.14	0.12	0.19
11th	0.32	0.16	0.37	**21th**	0.33	0.28	0.34

way, the performance results of conventional and proposed methods under unbalanced resistive loads are presented in Fig. 10. Considering the grid currents, it is clear that the magnitude values of phases are different for all cases. However, the proposed method provides balanced currents at the grid-side.

Fig. 11 shows the magnitudes of grid currents for the conventional/proposed method and clarifies the power flow balancing. In a conventional controlled system, the magnitudes of grid currents are dissimilar for all states. But, the currents are balanced for the proposed controlled system, and the magnitudes are approximately identical. The numerical values of grid currents for conventional/proposed are given in Table 3.

In an unbalanced situation, the signal consists of negative/zero sequence components in addition to the positive component. The magnitudes of negative sequence components for three-phase signals are the same, but they have 120-degree phase differences between each other. However, zero sequence components are the same for all phases. In this part, the negative sequence component (for only phase a) and the zero-sequence component of grid-side currents through conventional/proposed methods are presented in Fig. 12. As shown in results, the grid currents have negative/zero sequence components in the ratings of 5 A and 4 A, respectively. In contrast to the conventional method, the proposed method reduces negative/zero sequence to values less than 0.3 A.

In addition to negative/zero sequence component elimination, total harmonic distortion (THD) analysis has been carried out for three-phase grid currents. In harmonic spectrum analysis, THD values of grid currents are obtained as 1.47%, 1.45%, 1.49% for phase a, phase b, and phase c. According to the harmonic analysis, the obtained values that are less than power quality standards defined in IEEE 519 standards show the validity of the improved method. The THD values in percentage for each phase are given in Fig. 13. Also, the numerical values of harmonic components are given in Table 4.

5. Conclusion

The integration of renewable energy sources and electric grids is becoming more popular and more important day by day. Along with technological developments, the widespread use of renewable energy sources can be applied in different applications in the coming years. Furthermore, the increase in these energy sources' power capacities may also compensate for the various problems in modern applications. In this regard, the research works in the grid-interfaced hybrid energy systems are going to deal with the following topics: (1) the application in different custom power devices to solve voltage/current problems, (2) the implementation of high efficient improved power electronic interface, (3) integration with vehicle-to-grid (V2G) technology for charging management, and (4) overall system efficiency and reliability.

Unbalanced loads connected to the utility-systems distort the power balance at the grid-side and cause negative & zero sequence components at grid currents. For this purpose, an improved phase balancing method for grid inverter interfaced hybrid energy system is presented in this study. The proposed method has been built to generate individual references for each phase under unbalanced current conditions. For this, the current work has been constructed based on multiple αβ/dq frames instead of abc/dq frame. Moreover,

the proposed method is used in H-bridge inverters instead of three-phase three-wire inverters to compensate negative & zero sequence components at the grid-side. For a smooth operation, the controller consists of active/reactive power control, dc-link control and phase balancing control. In order to show the effectiveness of the presented method, the system is designed and tested in a Simulink environment program. In hybrid energy system, PV and FC are designed according to different irradiation/temperature operating conditions. In this way, four case studies with different power values are presented. The case studies show that the system supplies the controlled powers into grids/loads in order to ensure power stability at the grid-side. Also, the results show that unbalanced currents are compensated at the grid-side. The negative & zero sequence components at grid-currents are reduced significantly. In addition, the harmonic analysis of the injected currents is presented in order verify the validity of the proposed method.

Declaration of Competing Interest

The authors declare that they have no known competing financial interests or personal relationships that could have appeared to influence the work reported in this paper.

References

[1] İnci M. Interline fuel cell (I-FC) system with dual-functional control capability. Int J Hydrogen Energy 2019;45:891–903.
[2] İnci M. Active/reactive energy control scheme for grid-connected fuel cell system with local inductive loads. Energy 2020;197:117191.
[3] Aygen MS, İnci M. Performance results of photovoltaic/fuel cell based hybrid energy system under variable conditions. In: 2019 4th International Conference on Power Electronics and their Applications (ICPEA). p. 1–6.
[4] Bartolucci L, Cordiner S, Mulone V, Rossi JL. Hybrid renewable energy systems for household ancillary services. Int J Electr Power Energy Syst 2019;107:282–97.
[5] Aktas A, Erhan K, Özdemir S, Özdemir E. Dynamic energy management for photovoltaic power system including hybrid energy storage in smart grid applications. Energy 2018;162:72–82.
[6] Yuan Z, Wang W, Wang H. Optimal parameter estimation for PEMFC using modified monarch butterfly optimization. Int J Energy Res, vol. n/a.
[7] Priyadarshi N, Padmanaban S, Bhaskar MS, Blaabjerg F, Holm-Nielsen JB. An improved hybrid PV-wind power system with MPPT for water pumping applications. Int Trans Electrical Energy Syst 2020;30:e12210.
[8] García P, García CA, Fernández LM, Llorens F, Jurado F. ANFIS-based control of a grid-connected hybrid system integrating renewable energies, hydrogen and batteries. IEEE Trans Ind Inf 2014;10:1107–17.
[9] Selem SI, Hasanien HM, El-Fergany AA. Parameters extraction of PEMFC's model using manta rays foraging optimizer. Int J Energy Res 2020;44:4629–40.
[10] Bornapour M, Hooshmand R-A, Khodabakhshian A, Parastegari M. Optimal coordinated scheduling of combined heat and power fuel cell, wind, and photovoltaic units in micro grids considering uncertainties. Energy 2016;117:176–89.
[11] Fathima AH, Palanisamy K. 8 - Renewable systems and energy storages for hybrid systems. In: Fathima AH, Prabaharan N, Palanisamy K, Kalam A, Mekhilef S, Justo JJ, editors. Hybrid-Renewable Energy Systems in Microgrids. Woodhead Publishing; 2018. p. 147–64.
[12] Narendra Babu P, Chitti Babu B, Ranga Babu P, Gayadhar P. An optimal current control scheme in grid-tied hybrid energy system with active power filter for harmonic mitigation. Int Trans Electrical Energy Syst 2020;30:e12183.
[13] Fawzi M, El-Fergany AA, Hasanien HM. Effective methodology based on neural network optimizer for extracting model parameters of PEM fuel cells. Int J Energy Res 2019;43:8136–47.
[14] Athari H, Niroomand M, Ataei M. Review and Classification of Control Systems in Grid-tied Inverters. Renew Sustain Energy Rev 2017;72:1167–76.
[15] Pattnaik M, Kastha D. Unbalance and harmonic voltage compensation for a stand-alone variable speed constant frequency double-output induction generator supplying non-linear and unbalanced loads. IET Electr Power Appl 2013;7:27–38.
[16] Zhou Y, Nian H. Zero-sequence current suppression strategy of open-winding PMSG system with common DC bus based on zero vector redistribution. IEEE Trans Ind Electron 2015;62:3399–408.
[17] Ren HB, Wu Q, Gao WJ, Zhou WS. Optimal operation of a grid-connected hybrid PV/fuel cell/battery energy system for residential applications. Energy 2016;113:702–12.
[18] Elazab OS, Debouza M, Hasanien HM, Muyeen SM, Al-Durra A. Salp swarm algorithm-based optimal control scheme for LVRT capability improvement of grid-connected photovoltaic power plants: design and experimental validation. IET Renew Power Gener 2020;14:591–9.
[19] Belfedhal SA, Berkouk ELM, Messlem Y. Analysis of grid connected hybrid renewable energy system. J Renewable Sustainable Energy 2019;11.
[20] Maleki A, Hafeznia H, Rosen MA, Pourfayaz F. Optimization of a grid-connected hybrid solar-wind-hydrogen CHP system for residential applications by efficient metaheuristic approaches. Appl Therm Eng 2017;123:1263–77.
[21] Ramli MAM, Bouchekara HREH, Alghamdi AS. Optimal sizing of PV/wind/diesel hybrid microgrid system using multi-objective self-adaptive differential evolution algorithm. Renewable Energy 2018;121:400–11.
[22] Kim S, Jeon J, Cho C, Ahn J, Kwon S. Dynamic modeling and control of a grid-connected hybrid generation system with versatile power transfer. IEEE Trans Ind Electron 2008;55:1677–88.
[23] Housseini B, Okou AF, Beguenane R. Robust nonlinear controller design for on-grid/off-grid wind energy battery-storage system. IEEE Trans Smart Grid 2018;9:5588–98.
[24] Yi Z, Dong W, Etemadi AH. A unified control and power management scheme for PV-battery-based hybrid microgrids for both grid-connected and islanded modes. IEEE Trans Smart Grid 2018;9:5975–85.
[25] Çelik D, Meral ME, Inci M. Virtual Park-based control strategy for grid-connected inverter interfaced renewable energy sources. IET Renew Power Gener 2019;13:2840–52.
[26] Patra S, Ankur, Narayana M, Mohanty SR, Kishor N. Power quality improvement in grid-connected photovoltaic–fuel cell based hybrid system using robust maximum power point tracking controller. Electric Power Components Syst 2015;43:2235–50.
[27] Feng W, Sun K, Guan Y, Guerrero JM, Xiao X. A harmonic current suppression control strategy for droop-controlled inverter connected to the distorted grid. In: IEEE Energy Conversion Congress and Exposition (ECCE). p. 525–32.
[28] Fathabadi H. Utilizing solar and wind energy in plug-in hybrid electric vehicles. Energy Convers Manage 2018;156:317–28.
[29] Liao YH, Lai CM. Newly-constructed simplified single-phase multistring multilevel inverter topology for distributed energy resources. IEEE Trans Power Electron 2011;26:2386–92.
[30] Bayrak G, Cebeci M. Grid connected fuel cell and PV hybrid power generating system design with Matlab Simulink. Int J Hydrogen Energy 2014;39:8803–12.
[31] Micallef A, Apap M, Spiteri-Staines C, Guerrero JM. Mitigation of harmonics in grid-connected and islanded microgrids via virtual admittances and impedances. IEEE Trans Smart Grid 2017;8:651–61.
[32] Singaravel MMR, Daniel SA. MPPT with single DC–DC converter and inverter for grid-connected hybrid wind-driven PMSG–PV system. IEEE Trans Ind Electron 2015;62:4849–57.
[33] Aygen MS, İnci M. Zero-sequence current injection based power flow control strategy for grid inverter interfaced renewable energy systems. Energy Sources Part A 2020:1–22.
[34] Çelik D, Meral ME. Current control based power management strategy for distributed power generation system. Control Eng Pract 2019;82:72–85.
[35] Vandoorn TL, Van de Vyver J, Meersman B, Zwaenepoel B, Vandevelde L. Phase unbalance mitigation by three-phase damping voltage-based droop controllers in microgrids. Electr Power Syst Res 2015;127:230–9.
[36] İnci M, Buyuk M, Savrun MM, Demir MH. Design and analysis of fuel cell vehicle-to-grid (FCV2G) system with high voltage conversion interface for sustainable energy production. Sustainable Cities and Society 2021;67:. doi: https://doi.org/10.1016/j.scs.2021.102753102753.
[37] Büyük M, İnci M, Tan A, Tümay M. Improved instantaneous power theory based current harmonic extraction for unbalanced electrical grid conditions. Electr Power Syst Res 2019;177:106014.
[38] Buyuk M, Tan A, Tumay M, Bayindir KC. Topologies, generalized designs, passive and active damping methods of switching ripple filters for voltage source inverter: a comprehensive review. Renew Sustain Energy Rev 2016;62:46–69.
[39] Büyük M, Tan A, İnci M, Tümay M. A notch filter based active damping of LLCL filter in shunt active power filter. In: IEEE Ee2017 - International Symposium on Power Electronics (Ee); 2017, p. 1–6.
[40] Lakshmi M, Hemamalini S. Decoupled control of grid connected photovoltaic system using fractional order controller. Ain Shams Eng J Dec 2018;9:927–37.
[41] Yang B, Yu T, Shu HC, Zhu DN, An N, Sang YY, et al. Perturbation observer based fractional-order sliding-mode controller for MPPT of grid-connected PV inverters: design and real-time implementation. Control Eng Pract 2018;79:105–25.
[42] Soliman MA, Hasanien HM, Alkuhayli A. Marine predators algorithm for parameters identification of triple-diode photovoltaic models. IEEE Access 2020;8:155832–42.
[43] Qais MH, Hasanien HM, Alghuwainem S. Transient search optimization for electrical parameters estimation of photovoltaic module based on datasheet values. Energy Convers Manage 2020;214.
[44] Elazab OS, Hasanien HM, Alsaidan I, Abdelaziz AY, Muyeen SM. Parameter estimation of three diode photovoltaic model using grasshopper optimization algorithm. Energies 2020;13.
[45] Li Q, Chen WR, Liu ZX, Zhou GH, Ma L. Active control strategy based on vector-proportion integration controller for proton exchange membrane fuel cell grid-connected system. IET Renew Power Gener 2015;9:991–9.
[46] İnci M, Caliskan A. Performance enhancement of energy extraction capability for fuel cell implementations with improved Cuckoo search algorithm. Int J Hydrogen Energy 2020;45:11309–20.
[47] El-Fergany AA, Hasanien HM, Agwa AM. Semi-empirical PEM fuel cells model using whale optimization algorithm. Energy Convers Manage 2019;201:112197.

[48] Chen WR, Han Y, Li Q, Liu ZX, Peng F. Design of proton exchange membrane fuel cell grid-connected system based on resonant current controller. Int J Hydrogen Energy 2014;39:14402–10.
[49] Hajizadeh A, Golkar MA, Feliachi A. Voltage control and active power management of hybrid fuel-cell/energy-storage power conversion system under unbalanced voltage sag conditions. IEEE Trans Energy Convers 2010;25:1195–208.
[50] Aygen MS. Design, optimization and analysis of grid connected hybrid energy system under unbalanced loads MSc Thesis. Turkey: İskenderun Technical University, Hatay; 2020.
[51] Zakzouk NE, Abdelsalam AK, Helal AA, Williams BW. PV Single-phase grid-connected converter: DC-link voltage sensorless prospective. IEEE J Emerg Selected Top Power Electron 2017;5:526–46.
[52] İncİ M. Design and modeling of single phase grid connected fuel cell system. In: 2019 4th International Conference on Power Electronics and their Applications (ICPEA). p. 1–6.
[53] Pires VF, Cordeiro A, Foito D, Silva JF. Three-phase multilevel inverter for grid-connected distributed photovoltaic systems based in three three-phase two-level inverters. Sol Energy 2018;174:1026–34.
[54] Al-Shetwi AQ, Sujod MZ, Blaabjerg F. Low voltage ride-through capability control for single-stage inverter-based grid-connected photovoltaic power plant. Sol Energy 2018;159:665–81.

Mustafa İnci received the BSc and MSc degrees in Electrical-Electronics Engineering from Çukurova University, in 2011 and 2013. He received the PhD degree in Electrical-Electronics Engineering from Ç ukurova University, in 2017. He is currently Associate Professor at the department of Mechatronics Engineering, İskenderun Technical University. His research areas are advanced multilevel inverters, renewable energy systems, vehicle-to-grid (V2G) systems and custom power devices. He is a member of IEEE since 2015 and reviewer for IEEE, IET and Elsevier journals.

Mehmet Selim Aygen received the BSc degree in Electrical-Electronics Engineering from Çukurova University, Adana, in 2012. He received MSc degree in Electrical-Electronics Engineering from İskenderun Technical University, in 2020. He is currently continuing the PhD education in Electrical and Electronics Engineering from Gazi University. His research interests are industrial automation, hybrid energy systems and grid integration.